The challenging world of simple inorganic rings : revisiting Roesky's ketone and Roesky's sulfoxide

RESEARCH ARTICLE

The Challenging World of Simple Inorganic Rings: Revisiting Roesky's Ketone and Roesky's Sulfoxide

Ana V. Cunha,[a] Remco W.A. Havenith,[b][c] Christian Van Alsenoy,[a] and Frank Blockhuys*[a]

[a] Prof. Dr. Ana V. Cunha, Prof. Dr. Christian Van Alsenoy, Prof. Dr. Frank Blockhuys
Department of Chemistry
University of Antwerp
Groeneborgerlaan 171, B-2020 Antwerpen, Belgium
E-mail: frank.blockhuys@uantwerpen.be

[b] Prof. Dr. Remco W.A. Havenith
Stratingh Institute for Chemistry and Zernike Institute for Advanced Materials
University of Groningen
9747 AG Groningen, The Netherlands

[c] Prof. Dr. Remco W.A. Havenith
Department of Chemistry
Ghent University
Krijgslaan 281 (S3), B-9000 Gent, Belgium

Supporting information for this article is given via a link at the end of the document.

Abstract: The surprising differences between the experimental solid-state and calculated gas-phase structures of 5-oxo-1,3,2,4-dithiadiazole (Roesky's ketone, **1**) and 1-oxo-1,2,4,3,5-trithiadiazole (Roesky's sulfoxide, **2**), identified and studied in a series of papers published between 2004 and 2010 but then never satisfactorily explained, have been revisited, making use of the more advanced computational possibilities currently available. The previous calculations' considerable overestimations of the C–S and S–S bond lengths in **1** and **2**, respectively, have been partly explained based on the results of periodic calculations and the application of Valence Bond (VB) Theory. In the case of **1**, the crystal environment appears to stabilize a structure with a highly polarized C=O bond, which features a C–S bond with considerable double-bond character – an effect which does not exist for the isolated molecule – explaining the much shorter bond in the solid state. For **2**, a similar conclusion can be drawn for the S–S distance. For both compounds, though, packing effects are not the sole source of the differences: the inability of Density Functional Theory (DFT) to properly deal with the electronic structures of these apparently simple main-group systems remains a contributing factor.

Introduction

Even though sulfur-nitrogen chemistry is not a young research field – the first preparation of S_4N_4, one of the quintessential sulfur-nitrogen compounds, dates from 1835[1] – widespread interest in it started only after the 1975 discovery that polymeric $(SN)_x$, a one-dimensional pseudo-metal down to liquid helium temperature, starts behaving as a superconductor at 0.26 K.[2] Initially, the emphasis of sulfur-nitrogen chemistry (or chalcogen-nitrogen chemistry in general) was focused on fundamental studies, but, as a comparison of Tristram Chivers' original *Guide to Chalcogen-Nitrogen Chemistry*[3] and its updated version[4] shows, that focus has shifted during the last decade-and-a-half to the search for practical applications in fields as diverse as biological systems and materials science. Yet, due to the extreme diversity in the molecular structures of chalcogen-nitrogen compounds, they continue to present a challenge to chemical theory in general and their reactivity is not at all well understood.

Taking S_4N_4 and $(SN)_x$ polymer as examples, sulfur-nitrogen derivatives composed of alternating sulfur and nitrogen atoms connected by multiple bonds remain of special interest, forming an extensive set of chemical systems containing two topologically differing subsets – unsaturated chains and unsaturated cycles. All these systems are π-excessive, as the number of π-electrons exceeds the number of atomic centers: indeed, with each nitrogen atom supplying one and each sulfur atom supplying two π-electrons, a simple Molecular Orbital (MO) description leads to occupied antibonding π^*-levels in the ground state, and this thermodynamic destabilization is the cause of the observed structural diversity and the high and varied chemical reactivity.

One way to stabilize such systems is to enclose chains of a limited length in a ring, thus extending the π-delocalisation and stabilizing the heteroatomic fragment. 5-Oxo-1,3,2,4-dithiadiazole (**1**)[5] and 1-oxo-1,2,4,3,5-trithiadiazole (**2**),[6] both first prepared by Herbert Roesky in 1975 and later labeled "Roesky's ketone" (in 2004) and "Roesky's sulfoxide" (in 2006), respectively, can be considered prototypical representatives of the varied class of sulfur-nitrogen rings encompassing an $(SN)_2$ unit (Scheme 1).

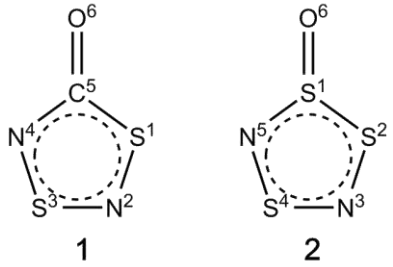

Scheme 1. Roesky's ketone (1) and Roesky's sulfoxide (2) with their atom numbering.

In the early 2000s an effort was undertaken to gain insight into the properties of the two compounds, using both experimental and computational techniques. The ketone's (**1**) molecular and solid-state structures, aromaticity and reactivity,[7] as well as its spectroscopic properties[8] were studied and it was observed that the calculated S(1)-C(5) distance of 1.941 Å (B3LYP/6-311+G*) was substantially longer than the experimental value obtained from a new single-crystal X-ray Diffraction (XRD) measurement, *i.e.*, 1.8305(17) and 1.8293(16) Å for each of the two molecules in the asymmetric unit. This surprising difference (an overestimation of about 0.112 Å), considerably larger than for the other ring bond lengths [0.002 Å for S(1)-N(2), 0.027 Å for N(2)-S(3), 0.020 Å for S(3)-N(4) and 0.021 Å for N(4)-C(5)] was then investigated further in two follow-up papers.

In the first, 16 functional/basis set combinations were evaluated, in addition to HF, MP2 and QCISD (the latter three with the 6-311+G* basis set).[9] Interestingly, taking the QCISD geometry as a benchmark, the original B3LYP/6-311+G* combination best reproduced the entire $(SN)_2$ fragment, albeit with a very poor S-C distance. Any attempt to improve the latter (B3LYP/cc-pCVQZ brought it down, but only to 1.890 Å) always resulted in a poorer description of the rest of the ring.

In the second, another 12 functional/basis set combinations were added, together with calculations at the MP4(SDQ), CCSD and CCSD(T) levels of theory, the latter two with basis sets up to cc-pV(T+d)Z.[10] Taking two structural criteria, based on structural trends seen in the solid-state geometry, as benchmarks, the MP4(SDQ)/aug-cc-pVTZ combination came out best overall, with a less unacceptable S(1)-C(5) distance of 1.845 Å; the latter is equal to that of the best DFT combination (B1B95/aug-pc3). Based on this approach, it was concluded that even the CCSD(T)/cc-pV(T+d)Z geometry with an S(1)-C(5) distance of 1.858 Å was unacceptable.

One of the main difficulties in these studies was finding the proper benchmark with which to evaluate each of the computational methods: the lack of an experimental gas-phase structure forced us to use the results of an, at the time, high-level computational method (QCISD), or to revert to structural trends seen in the only available experimental geometry, questionable choices made ultimately due to the computational limitations of the day. Some years later, the rotational spectrum of Roesky's ketone (**1**) was measured and based on it the computational data were re-evaluated.[11] The analysis indicated that MP4(SDQ)/aug-cc-pVTZ, MP4(SDQ)/cc-pVTZ, B3PW91/cc-pV(T+d)Z and mPW1PW91/aug-cc-pVTZ produce rotational constants which deviate (rms difference) from the experimental values by less than about 7 MHz, the latter value being associated with the solid-state geometry; it was noted that these combinations outperformed CCSD(T)/cc-pV(T+d)Z, for which an rms difference of 26 MHz was obtained. The associated S(1)-C(5) distances are 1.845, 1.849, 1.872 and 1.867 Å, respectively, none of which are quite impressive. Remarkably, the good fit between the experimental rotational constants and those obtained from the solid-state geometry suggested that the structure in the gas phase must closely resemble that in the solid, but the calculations seemed to disagree.

The situation was even more complex for Roesky's sulfoxide (**2**), particularly from a computational point of view considering the presence of a third sulfur atom. Before it was subjected to a structural, bonding, aromaticity and reactivity study, in which a new experimental solid-state geometry was published,[12] the computational challenges were investigated.[13] As expected, the S(1)-S(2) distance, with a value of 2.2158(9) Å in the solid, was the main source of problems. The results from 19 combinations of wave-function-based methods and 24 combinations of functionals with a variety of basis sets [up to CCSD(T)/6-311G* and CCSD/cc-pVTZ] were evaluated. The latter combination was used as benchmark, even though, with an S(1)-S(2) distance of 2.233 Å, it was not a very impressive one. B1B95/aug-cc-pVTZ was found as best DFT combination overall, but it could not do better than 2.263 Å for S(1)-S(2). The calculated S-S distance closest to the experimental value came from MP4(SDQ)/aug-cc-pVTZ (2.228 Å) and B1B95/aug-cc-pVQZ (2.255 Å). Again, CCSD(T) performed poorly (2.409 Å), but in this case the small basis set (chosen out of necessity) was cited as the reason. All in all, just like its carbon analogue, the sulfoxide and its molecular structure seemed to represent a considerable computational challenge.

It may be clear that, in the absence of the proper experimental benchmark, the computational possibilities of the time were too limited to reach any final conclusion: going beyond CCSD(T) with a large enough basis set was out of the question and methods to calculate the properties of the solid state at any acceptable level of theory were unavailable. Furthermore, the assumption up to then had been that the difference between solid state and gas phase should not be too large (as suggested by the rotational data), even though there may be packing effects causing just that. Considering the advances that have been made during the past 15 years, particularly in terms of the development of computer codes for fast calculations on infinite systems, we decided to continue our search for a proper description of Roesky's ketone (**1**) and Roesky's sulfoxide (**2**), and this is the subject of the current paper. The results from calculations of the crystal structure of both compounds under Periodic Boundary Conditions have been combined with those from Valence Bond (VB) Theory, (i) to verify whether the experimental solid-state geometries can be reproduced, and (ii), if so, to ascertain the particular effects of the packing on the molecular structures that could explain a potentially significant difference between solid state and gas phase.

Table 1. Interatomic distances (in Å) for Roesky's ketone (**1**), calculated in various environments, together with the experimental solid-state values for both molecules in the asymmetric unit.

	S(1)-N(2)	N(2)-S(3)	S(3)-N(4)	N(4)-C(5)	S(1)-C(5)	C(5)-O(6)
XRD molecule 1	1.6395(14)	1.5807(15)	1.5763(15)	1.386(2)	1.8305(17)	1.211(2)
XRD molecule 2	1.6425(15)	1.5814(15)	1.5750(16)	1.384(2)	1.8293(16)	1.211(2)
1 with BAND	1.627	1.589	1.568	1.374	1.891	1.194
1 with ADF	1.630	1.594	1.572	1.374	1.918	1.196
1 in crystal	1.626	1.583	1.579	1.367	1.845	1.214
1 in cluster	1.626	1.585	1.586	1.366	1.867	1.219

Results and Discussion

Since our last publication[12] an additional 109 sets of functional/ basis set combinations for each of the two compounds has been added and the associated geometrical parameters have been compiled in Tables S1 and S2 in the Supporting Information for **1** and **2**, respectively, together with the DFT results from refs. 9 and 10, and ref. 13, respectively.

For Roesky's ketone (**1**) (Table S1), it is interesting to note that almost any conceivable S(1)-C(5) distance can be found in the range between 1.813 and 2.179 Å, depending on which combination is used. The other four ring distances are likewise found in fairly large ranges but these are about three times smaller than that for S(1)-C(5) (0.366 Å): 0.036 Å for N(4)-C(5), 0.058 Å for S(1)-N(2), 0.114 Å for S(3)-N(4) and 0.129 Å for N(2)-S(3). A variety of combinations now produce S-C distances which are shorter than the experimental ones, as low as 1.813 Å for BHandH/cc-pVQZ.

For Roesky's sulfoxide (**2**) (Table S2), the range of S(1)-S(2) distances is a staggering 0.471 Å (from 2.168 to 2.639 Å), four times larger than for the other four bonds: 0.056 Å for S(2)-N(3), 0.079 Å for N(5)-S(1), 0.119 Å for N(3)-S(4) and 0.117 Å for S(4)-N(5). Here too, S-S distances shorter than the experimental one, down to 2.168 Å for ωB97/cc-pVQZ, are produced.

Roesky's Ketone

The geometry of **1** was re-optimized using different approaches and the results have been presented in Table 1. As a reference, an isolated molecule of **1** was optimized with the periodic code BAND in a PBC cell using the r^{2}SCAN-D4 functional combined with the TZ2P basis set producing, unsurprisingly, results similar to the previously mentioned molecular calculations. The S(1)-C(5) bond length is 1.891 Å, a bit shorter than that obtained for an isolated molecule with the molecular code ADF, using the same functional and basis set, *i.e.*, 1.918 Å; note that this difference is considerably larger than for the five other bonds (Table 1).

When the atom positions were optimized in the experimentally determined unit cell (*i.e.*, without optimizing the cell parameters), using the same method, a significant shortening of the S(1)-C(5) bond length to 1.845 Å was found, a value which is in much better agreement with the experimental values of 1.8305(17) and 1.8293(16) Å. Apparently, crystal packing effects play a key role in determining the S(1)-C(5) bond length. The other bond lengths in the crystal structure are in excellent agreement with those of "**1** with BAND" and "**1** with ADF", except for C(5)-O(6), which is somewhat longer but closer to the experimental values. Therefore, not only the S-C but also the C=O bond seems to be very sensitive to effects of the molecular environment.

In order to elucidate how the environment affects the latter two bonds a geometry optimization of **1** embedded in a cluster of 18 molecules (a cluster generated from the optimized crystal structure, with one central molecule surrounded by its 18 nearest neighbours) was performed, without PBC. In this cluster too a contraction of the S(1)-C(5) bond length is seen, to 1.867 Å, but this value is again larger than in the optimized crystal geometry and, consequently, larger than the experimental values; C(5)-O(6) has also increased, but negligibly so.

Table 2. The contributions to the bonding energy (in kcal.mol^{-1}) of the central molecule of **1** within a cluster of 18 molecules.

Decomposition	Contribution
E_{Pauli}	32.44
E_{elstat}	–37.86
E_{orb}	–21.43
E_{disp}	–13.03
E_{bond}	–39.88

To further analyze this observation an Energy Decomposition Analysis (EDA) was performed with the central molecule as one fragment, and the other cluster molecules as the second fragment. The bonding energy (E_{bond}) was found to be –39.88 kcal.mol^{-1} (Table 2). Surprisingly, the contributions from the electrostatic

(E_{elstat}) and orbital interactions (E_{orb}) are relatively large, and the smallest contribution to the bonding comes from dispersion effects (E_{disp}), even though it is a molecular crystal. The large electrostatic component suggests a large dipole-dipole interaction, while the orbital contribution suggests that the molecule is polarized by the crystal embedding.

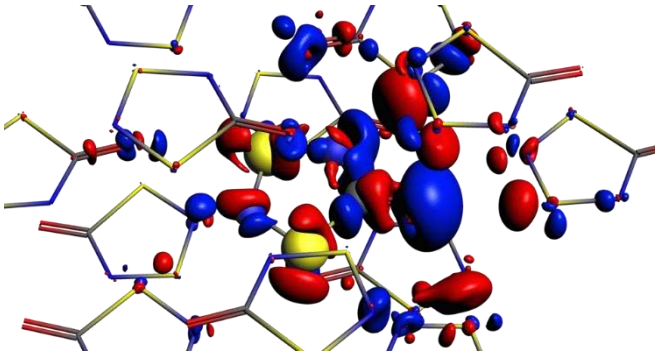

Figure 1. Difference in density [$\Delta\rho = \rho_{cluster} - (\rho_{mol} + \rho_{embed})$] upon addition of the central molecule (isosurface 0.003); blue is positive, indicating an increase in electron density, and red is negative, indicating a decrease in electron density.

To assess how **1** is polarized due to the embedding, the electron density difference between the total electron density of the cluster and the sum of the densities of the isolated fragments (the density of the central molecule, ρ_{mol}, and the density of the embedding cluster of 18 molecules, ρ_{embed}) was calculated and it has been plotted in Figure 1: blue indicates regions where the electron density increases upon complex formation, while red indicates regions where the electron density decreases. Figure 1 shows that electron density shifts towards the carbonyl oxygen atom in the central molecule, thus making this oxygen atom slightly more negative than in the isolated molecule.

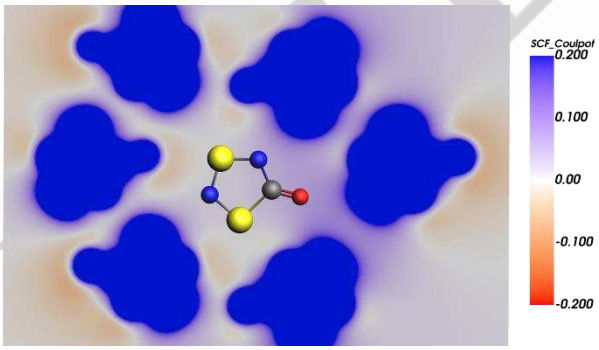

Figure 2. Electrostatic potential plotted in the plane of the central molecule, calculated in a cluster of molecules, without the central molecule.

The occurrence of this shift in electron density can be explained by considering the electrostatic potential, generated by the embedding molecules, at the position of this oxygen atom (Figure 2). The electrostatic potential map shows that the embedding molecules generate a slightly positive environment at the position of the carbonyl oxygen atom. This positive environment can stabilize a higher negative charge on that atom, which, consequently, promotes a shift of electron density in the direction of the carbonyl oxygen atom.

To further assess the effect on the geometry of a positively charged environment around the carbonyl oxygen, the geometry of **1** was optimized with a nearby point charge, and the variation of the bond lengths was plotted as a function of the magnitude of the positive charge (Figure 3). The plot shows that the three S-N bond lengths are nearly unaffected by the size of the positive point charge, that the C-N and C-O distances slighty decrease and increase, respectively, but that the S-C bond length is greatly affected: it considerably decreases with the increasing positive point charge size which would stabilize a negative charge localized on the carbonyl oxygen atom.

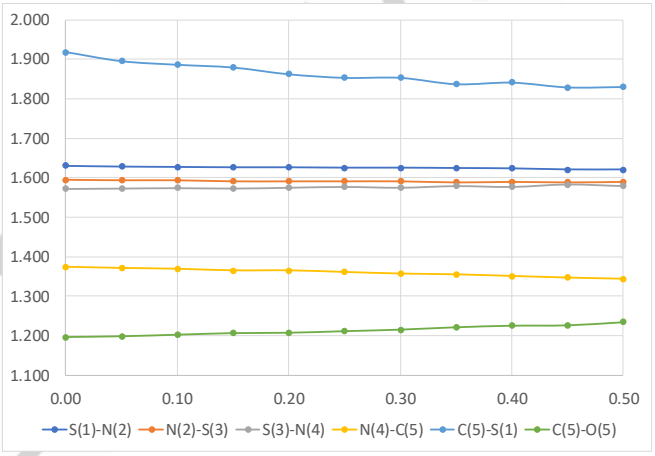

Figure 3. Variation of the bond lengths (in Å) as a function of the magnitude of a positive point charge in the vicinity of the carbonyl oxygen atom.

The hypothesis that a positive charge (or positive embedding environment) stabilizes resonance structures with a negative charge on the oxygen atom was further corroborated with Valence Bond (VB) calculations. The cumulative weights of the structures with a C=O double bond (**A**) on the one hand, and those with an aromatic 6π-electron positively charged five-membered ring with a C–O^- single bond (**B**) on the other, are depicted in Figure 4. The total weight of the ionic aromatic structures (**B**) is 0.139. This weight increases to 0.327 when a point charge of +0.2 is placed in the vicinity of O(6), indicating an increase in aromaticity of the five-membered ring, which leads to more double bond character between S(1) and C(5). This increase in double bond character is the cause of the shortening of this bond length in the environment. Hence, the poor agreement for the bond lengths of **1** obtained from gas-phase calculations with the experimental XRD structure is not only caused by the inherently difficult electronic structure of **1**, but also because of missing environment effects, which have a strong influence on the S(1)-C(5) bond length in particular.

Table 3. Interatomic distances (in Å) for Roesky's sulfoxide (**2**), calculated in various environments, together with the experimental solid-state values.

	S(1)-S(2)	S(2)-N(3)	N(3)-S(4)	S(4)-N(5)	N(5)-S(1)	S(1)-O(6)
XRD	2.2158(9)	1.6372(18)	1.5689(19)	1.5827(18)	1.6447(16)	1.4769(17)
2 with BAND	2.340	1.617	1.571	1.582	1.640	1.459
2 in crystal	2.275	1.622	1.564	1.587	1.640	1.479

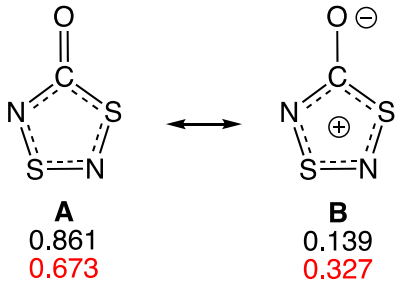

Figure 4. The cumulative weights of valence bond structures of 1 with a C=O moieity (A) or a C–O⁻ moieity (B). The weights in black are the gas-phase weights, the ones in red are calculated with a point charge of +0.2 near the carbonyl oxygen atom.

Roesky's Sulfoxide

The geometry of **2** was re-optimized using just two of the approaches applied for **1** and the results have been presented in Table 3. As a reference, an isolated molecule of **2** was optimized with the periodic code BAND in a PBC cell using the r^{2}SCAN-D4 functional combined with the TZ2P basis set, producing a poor overall geometry, comparable to all other DFT geometries.

When the atom positions were optimized in the experimentally determined unit cell (*i.e.*, without optimizing the cell parameters), using the same method, a significant shortening of the S(1)-S(2) bond length to 2.275 Å was found, a value which is in much better agreement with the experimental value of 2.2158(9) Å. The S=O distance too has clearly evolved in the right direction, supporting the idea that for **2** the same crystal packing effects are at play as those found for Roesky's ketone (**1**).

Conclusion

The above described extension of our previous work on the two sulfur-nitrogen compounds under investigation leads to a number of new insights. (i) The general problems DFT has with properly describing the electronic structures of these systems, previously identified as the *overestimation* of the S(1)-C(5) distance in **1** and the S(1)-S(2) distance in **2**, have been expanded by observing that, even though the large majority of functionals do overestimate these distances, a non-negligible number of them *underestimate* the bond lengths. Consequently, choosing a functional/basis set combination to calculate their molecular properties remains a particularly challenging task. (ii) For a given combination of functional and basis set, it has now become clear that the crystal packing has a definite and specific influence on the molecular structure: the surrounding molecules generate an electronic environment which leads to a shift of electron density in the direction of the oxygen atom. This reshuffling of electron density then leads to a considerable shortening of the C-S bond in **1** and the S-S bond in **2**.

This then begs the question of how "wrong" the gas-phase geometries are which were obtained with the highest-level methods in our previous work, *i.e.*, CCSD(T)/cc-pV(T+d)Z for **1** and CCSD/cc-pVTZ for **2**, as there is no more reason for gas-phase and solid-state structures to be similar. Indeed, these geometries may be quite close to the "real" gas-phase structures, but only if, in contrast to DFT, CCSD(T) *is* capable of properly describing the rings' electronic structures. In the absence of an experimental gas-phase geometry, this can only be verified by assessing the quality of a CCSD(T)-level calculation of the solid-state structures of **1** and **2**. As this is beyond our computational possibilities at this moment, we are again faced with at least one remaining unanswered question.

Computational Methods

Geometries presented in the main text were optimized with ADF[14-16] and BAND[17] (as implemented in the AMS2022 suite) using the built-in TZ2P basis set and r^{2}SCAN-D4 functional.[18] Energy Decomposition Analyses were also performed with ADF.[19] Hessian calculations were performed to confirm that all optimized structures are genuine minima at this level of theory. Scalar relativistic effects were included via the ZORA method.[20-22] In calculations labelled "in crystal" the atom positions were optimized in the experimentally determined unit cell, without optimizing the cell parameters, applying the default regular *k*-space grids, *i.e.*, a 1 × 1 × 3 grid for **1** and a 3 × 3 × 3 grid for **2**; in the calculation labelled "in cluster" one central molecule was surrounded by its 18 nearest neighbours identified from the optimized crystal structure. To generate the data in Figure 3 a point charge was placed 0.97 Å from the carbonyl oxygen atom on the normal to the molecular plane through that atom. Valence bond SCF calculations[23,24] were performed with TURTLE,[25,26] as implemented in GAMESS-UK.[27] For the Valence Bond calculations, the 6-311G** basis set was used. Basis sets were

taken from the BasisSet Exchange Library.[28-30] Only the π-orbitals were taken into consideration, the σ-orbitals were taken from a preceding Hartree-Fock calculation and were kept frozen. The active orbitals were kept strictly atomic. The Gallup and Norbeck scheme[31] is used to calculate the weights of the individual, non-orthogonal, VB structures. The advantage of these weights is that they are always positive and sum to 1. Geometries presented in the Supporting Information were optimized using the Gaussian09 suite of programs;[32] the functionals and basis sets were used as they are implemented in the program.

Supporting Information

Table S1 and Table S2 contain the DFT geometries of **1** and **2**, respectively, and Tables S3-S7 contain the Cartesian coordinates associated with the calculations presented in Tables 1 and 3.

Acknowledgements

This research used resources (Summit) of the Oak Ridge Leadership Computing Facility at the Oak Ridge National Laboratory, which is supported by the Office of Science of the U.S. Department of Energy under Contract No. DE-AC05-00OR22725 (DD). This work was sponsored by NWO Exact and Natural Sciences for the use of supercomputer facilities (EINF-431 and contract no. 17197 7095). RWAH and AVC thank S. Dolas (SURF, NL) for allowing us to perform calculations on the experimental AMD platform kleurplaat maintained and operated by SURF Open Innovation Lab. We would like to thank the Center for Information Technology of the University of Groningen for their support and for providing access to the Peregrine/Habrok high performance computing cluster.

Keywords: dithiadiazole • trithiadiazole • molecular geometry • solid-state geometry • valence bond theory

[1] M. Gregory, *J. Pharm.* **1835**, *21*, 315.

[2] R. L. Greene, G. B. Street, L. J. Suter, *Phys. Rev. Lett.* **1975**, *34*, 577.

[3] T. Chivers, *A Guide to Chalcogen-Nitrogen Chemistry*, World Scientific, New Jersey, **2005**.

[4] T. Chivers, R. S. Laitinen, *Chalcogen-Nitrogen Chemistry – From Fundamentals to Applications in Biological, Physical and Materials Sciences*, World Scientific, New Jersey, **2022**.

[5] H. W. Roesky, E. Wehner, *Angew. Chem. Int. Ed. Eng.* **1975**, *14*, 498.

[6] H. W. Roesky, H. Wiezer, *Angew. Chem. Int. Ed. Eng.* **1975**, *14*, 258.

[7] J. Van Droogenbroeck, K. Tersago, C. Van Alsenoy, S. M. Aucott, H. L. Milton, J. D. Woollins, F. Blockhuys, *Eur. J. Inorg. Chem.* **2004**, 3798.

[8] K. Tersago, J. Van Droogenbroeck, C. Van Alsenoy, W. A. Herrebout, B. J. van der Veken, S. M. Aucott, J. D. Woollins, F. Blockhuys, *Phys. Chem. Chem. Phys.* **2004**, *6*, 5140.

[9] J. Van Droogenbroeck, K. Tersago, C. Van Alsenoy, F. Blockhuys, *Chem. Phys. Lett.* **2004**, *399*, 516.

[10] K. Tersago, J. Oláh, J. M. L. Martin, T. Veszprémi, C. Van Alsenoy, F. Blockhuys, *Chem. Phys. Lett.* **2005**, *413*, 440.

[11] F. Blockhuys, K. Tersago, S. A. Shlykov, A. Konrad, D. Christen, *J. Mol. Struct.* **2010**, *978*, 147.

[12] K. Tersago, V. Matuska, C. Van Alsenoy, A. M. Z. Slawin, J. D. Woollins, F. Blockhuys, *Dalton Trans.* **2007**, 4529.

[13] K. Tersago, C. Van Alsenoy, J. D. Woollins, F. Blockhuys, *Chem. Phys. Lett.* **2006**, *423*, 422.

[14] E. J. Baerends, ADF 2017.01, SCM, Theoretical Chemistry, Vrije Universiteit Amsterdam, Amsterdam (The Netherlands), **2017**.

[15] C. Fonseca Guerra, J. G. Snijders, G. te Velde, E. J. Baerends, *Theor. Chem. Acc.* **1998**, *99*, 391.

[16] G. te Velde, F. M. Bickelhaupt, E. J. Baerends, C. Fonseca Guerra, S. J. A. van Gisbergen, J. G. Snijders, T. Ziegler, *J. Comput. Chem.* **2001**, *22*, 931.

[17] (a) G. te Velde, E. J. Baerends, *Phys. Rev. B* **1991**, *44*, 7888; (b) BAND 2023.1, SCM, Theoretical Chemistry, Vrije Universiteit Amsterdam, Amsterdam (The Netherlands). (c) E. S. Kadantsev, R. Klooster, P. L. de Boeij, T. Ziegler, *Mol. Phys.* **2007**, *105*, 2583.

[18] S. Ehlert, U. Huniar, J. Ning, J. W. Furness, J. Sun, A. D. Kaplan, J. P. Perdew, J. G. Brandenburg, *J. Chem. Phys.* **2021**, *154*, 061101.

[19] F. M. Bickelhaupt, E. J. Baerends in *Reviews in Computational Chemistry, Vol. 15* (Eds.: K. B. Lipkowitz, D. B. Boyd), Wiley-VCH, New York, **2000**, pp. 1-86.

[20] E. van Lenthe, E. J. Baerends, J. G. Snijders, *J. Chem. Phys.* **1993**, *99*, 4597.

[21] E. van Lenthe, E. J. Baerends, J. G. Snijders, *J. Chem. Phys.* **1994**, *101*, 9783.

[22] E. van Lenthe, R. van Leeuwen, E. J. Baerends, J. G. Snijders, *Int. J. Quantum Chem.* **1996**, *57*, 281.

[23] J. H. van Lenthe, G. G. Balint-Kurti, *Chem. Phys. Lett.* **1980**, *76*, 138.

[24] J. H. van Lenthe, G. G. Balint-Kurti, *J. Chem. Phys.* **1983**, *78*, 5699.

[25] J. H. van Lenthe, F. Dijkstra, R. W. A. Havenith in *Valence Bond Theory, Vol. 10* (Ed.: D. L. Cooper), Elsevier, Amsterdam, **2002**, pp. 79-112.

[26] J. Verbeek, J. H. Langenberg, C. P. Byrman, F. Dijkstra, R. W. A. Havenith, J. J. Engelberts, M. Zielinski, Z. Rashid, J. H. van Lenthe, TURTLE, an ab initio VB/VBSCF program, Utrecht, The Netherlands, **1988-2016**.

[27] M. F. Guest, I. J. Bush, H. J. J. van Dam, P. Sherwood, J. M. H. Thomas, J. H. van Lenthe, R. W. A. Havenith, J. Kendrick, *Mol. Phys.* **2005**, *103*, 719.

[28] D. Feller, *J. Comput. Chem.* **1996**, *17*, 1571.

[29] B. P. Pritchard, D. Altarawy, B. Didier, T. D. Gibsom, T. L. Windus, *J. Chem. Inf. Model.* **2019**, *59*, 4814.

[30] K. L. Schuchardt, B. T. Didier, T. Elsethagen, L. Sun, V. Gurumoorthi, J. Chase, J. Li, T. L. Windus, *J. Chem. Inf. Model.* **2007**, *47*, 1045.

[31] G. A. Gallup, J. M. Norbeck, *Chem. Phys. Lett.* **1973**, *21*, 495.

[32] M. J. Frisch, G. W. Trucks, H. B. Schlegel, G. E. Scuseria, M. A. Robb, J. R. Cheeseman, G. Scalmani, V. Barone, B. Mennucci, G. A. Petersson, H. Nakatsuji, M. Caricato, X. Li, H. P. Hratchian, A. F. Izmaylov, J. Bloino, G. Zheng, J. L. Sonnenberg, M. Hada, M. Ehara, K. Toyota, R. Fukuda, J. Hasegawa, M. Ishida, T. Nakajima, Y. Honda, O. Kitao, H. Nakai, T. Vreven, J. A. Montgomery, Jr., J. E. Peralta, F. Ogliaro, M. Bearpark, J. J. Heyd, E. Brothers, K. N. Kudin, V. N. Staroverov, R. Kobayashi, J. Normand, K. Raghavachari, A. Rendell, J. C. Burant, S. S. Iyengar, J. Tomasi, M. Cossi, N. Rega, J. M. Millam, M. Klene, J. E. Knox, J. B. Cross, V. Bakken, C. Adamo, J. Jaramillo, R. Gomperts, R. E. Stratmann, O. Yazyev, A. J. Austin, R. Cammi, C. Pomelli, J. W. Ochterski, R. L. Martin, K. Morokuma, V. G. Zakrzewski, G. A. Voth, P. Salvador, J. J.

Dannenberg, S. Dapprich, A. D. Daniels, O. Farkas, J. B. Foresman, J. V. Ortiz, J. Cioslowski, D. J. Fox, Gaussian 09, Revision A.02, Gaussian, Inc., Wallingford CT, **2009**.

Entry for the Table of Contents

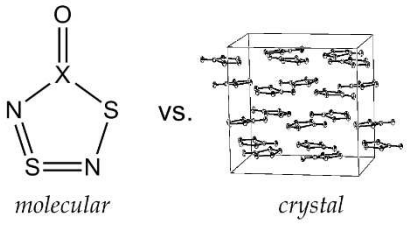

Performing Molecular Orbital calculations on unsaturated sulfur-nitrogen rings remains a challenging task. One particular unresolved issue was the large difference between the experimental solid-state geometries and the gas-phase geometries of two five-membered ring systems, calculated by a variety of methods including DFT, MP4(SDQ) and CCSD(T). New solid-state and Valence Bond calculations present a partial explanation, even though a full final answer fails to emerge.